PRELIMINARY DESIGN OF THE BEAM POSITION DETECTORS FOR THE FERMILAB MAIN INJECTOR

E. Barsotti, Jr. and J. Crisp
Fermi National Accelerator Laboratory, Batavia, IL 60510*

ABSTRACT

The progress of the design of the 204 detectors required for the Fermilab Main Injector, (FMI), Beam Position Monitor, (BPM), system is described. To conserve space, the detectors will be located inside the quadrupole magnets. The output from four striplines shorted at one end will be combined to form either horizontal or vertical detectors. Commercially available software was used to select the geometry of the striplines for desired characteristic impedance, linearity, and output power. Prototype measurements are shown to agree with simulation and mechanical issues are discussed.

INTRODUCTION

The Fermilab Main Injector is being constructed to replace the Main Ring and increase the luminosity of colliding beams in the Tevatron. The FMI will provide 150

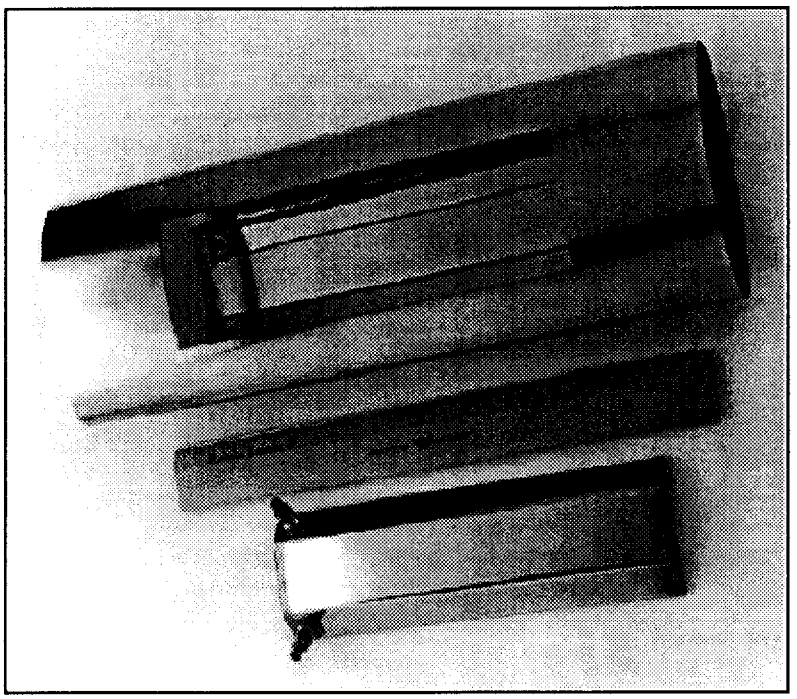

Figure 1. The FMI BPM Detector prototype, with one vacuum enclosure removed.

* Operated by the Universities Research Association under contract with the U. S. Dept. of Energy

GeV protons and antiprotons to the Tevatron, 120 GeV protons for antiproton production, and support fixed target experiments. The range of intensity for multibunch batches is 1E9 to 8E10 particles per bunch, (ppb), while coalesced single bunches are expected to reach 3E11 ppb[1,2].

Each FODO cell in the FMI requires two BPM detectors, horizontal at the focusing quad and vertical at the defocusing quad. The Main Ring quadrupoles are being reused and the FMI beam pipe geometry was chosen to fit inside them[3]. The detectors will be constructed from this beam pipe and are designed to fit inside the quadrupole, (see Figures 1 and 2). The desired position range is ±20 mm in both the horizontal and vertical planes. Five wide aperture detectors are used to accommodate the closed orbit positions required by restricted apertures at the Lambertson magnets. Space is available at these locations allowing the use of Booster style BPM's mounted external to the quadrupoles.

The detector is formed from 4 transmission line strips, or striplines, located on the perimeter of the beam pipe, (Figure 2). The characteristic impedance of 50Ω is determined by the gap between the strip and the beam pipe. Each stripline is shorted at one end and connected to an SMA ceramic feedthrough at the other. The outputs will be combined in pairs externally to form either a horizontal or vertical detector. The detector will be non-directional because one end of the stripline is shorted. This design does not require separate horizontal and vertical detectors.

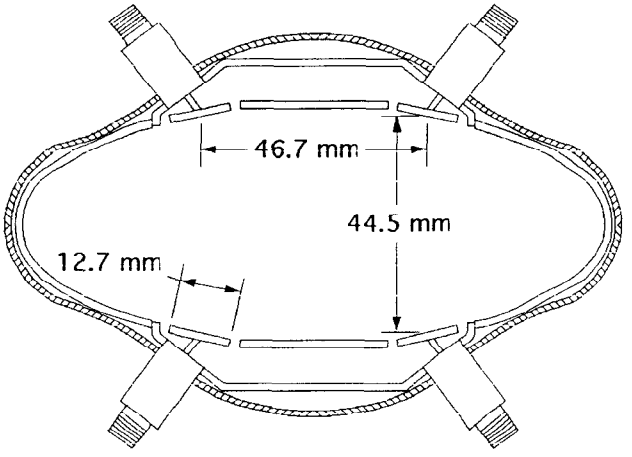

Figure 2. Cross section of the FMI BPM detector and enclosure prototype, inside the MR/FMI quadrupole pipe.

MECHANICAL DESIGN

The decision to place the detectors inside the quadrupoles had a strong influence on their design. The limited space between the FMI beam pipe and the quadrupole precludes placing electrodes on the horizontal axis without restricting the aperture. The horizontal separation of the plates is also limited.

The first attempt to realize the plate geometry consisted of cutting the plates into the beam pipe itself using a wire cutting EDM. The residual forces from forming the elliptical pipe caused the strips to bow outwards making this technique impractical. It was thought that annealing the pipe prior to cutting would not cure the problem.

The second approach was to use the wire EDM to cut 4 rectangles out of the FMI beam pipe and weld the striplines in place. This worked well enough to verify the simulations of characteristic impedance, sensitivity, linearity, and resolution of the 4 stripline geometry. However, as the pipe was cut, the elliptical shape changed making it difficult to cut a straight line and the resulting geometry changed along the length of the cutouts.

The second prototype consisted of making an upper and lower plate assembly which gets welded to a beam pipe with the appropriate cutout. Each assembly consists of a cover piece bent from sheet metal, two end plates, two striplines, two feedthroughs, and a ground plate positioned between the striplines, (see Figures 1 and 2). The end plates have slots machined in them to position the assembly in the pipe and hold the striplines in position to insure the correct characteristic impedance. The end with feedthroughs extends from the quadrupole by just enough to allow cable connections.

ELECTRICAL DESIGN

The final dimensions of the striplines in the detectors were determined by optimizing the electrical properties under the mechanical constraints. Detector electrical issues include linearity, sensitivity, beam impedance, and characteristic impedance. Other issues include dynamic range and resolution but involve the processing electronics.

The detector properties can be numerically simulated using commercially available software from Artech House[4], "Matrix Parameters for Multiconductor Transmission Lines". This DOS-based moment method code solves the 2-D transmission line matrices and electrostatic charge distributions for a standard transmission line configuration, (e.g., microstrip or coplanar) or a user-defined geometry, as was done here. The 249 points defining the cross section of the structure were obtained from the CAD drawing of the detector.

The charge density induced by the beam on the inside surface of the beam pipe is calculated by modeling the geometry as a coaxial transmission line. The beam is assumed to be a small diameter center conductor with the beam pipe forming the outer conductor. The image charge distribution on the pipe is essentially the same as the distribution for highly relativistic beam. If the gaps between the striplines and the beam pipe are small, the charge on the strip can be found by integrating the charge over its location. A number of charge distributions were obtained for beam position steps of 5 mm covering one quadrant of the detector. An in-house post-processing program extracted the total charge on each strip for every position and calculated the output power at the BPM processing frequency using the following equation.[5]

$$P(m\omega_0) = \frac{V^2(m\omega_0)}{2Z_0}, \qquad V(m\omega_0) \cong 2FZ_0\langle I_b\rangle \exp\left(-\frac{m^2\omega_0^2\sigma^2}{2}\right)\sin\left(\frac{m\omega_0 l}{c}\right) \tag{1}$$

The results are presented in Figure 3 for 1E9 ppb and a full ring of bunches having length σ = 2 nsec. The fraction of charge on the strip is F, the average or dc beam current is $\langle I_b \rangle$, the frequency $m\omega_0$ is 2π 53.1 MHz, the stripline length l is 20 cm, and the characteristic impedance Z_0 is 50Ω. The detector dimensions are provided in Figure 2.

	#1	#2	#3	#4
0,0	-30.23	-30.23	-30.23	-30.23
5,0	-27.89	-32.8	-32.8	-27.89
10,0	-25.9	-35.53	-35.53	-25.9
15,0	-24.46	-38.39	-38.39	-24.46
20,0	-23.78	-41.38	-41.38	-23.78
25,0	-24.07	-44.54	-44.53	-24.07
0,5	-29.23	-29.24	-31.95	-31.95
5,5	-26.41	-32.18	-34.22	-29.96
10,5	-23.85	-35.2	-36.71	-28.37
15,5	-21.85	-38.27	-39.39	-27.29
20,5	-20.77	-41.45	-42.27	-26.87
25,5	-20.97	-44.76	-45.36	-27.24
0,10	-29.16	-29.16	-34.42	-34.41
5,10	-25.71	-32.56	-36.47	-32.7
10,10	-22.31	-35.9	-38.8	-31.39
15,10	-19.37	-39.24	-41.38	-30.59
20,10	-17.56	-42.65	-44.23	-30.41
25,10	-17.61	-46.22	-47.37	-30.94
0,15	-30.61	-30.61	-38.01	-38.02
5,15	-26.44	-34.47	-39.92	-36.51
10,15	-21.84	-38.16	-42.19	-35.46
15,15	-17.18	-41.84	-44.81	-34.96
20,15	-13.92	-45.63	-47.79	-35.11
25,15	-13.5	-49.68	-51.28	-36.05
0,20	-35.31	-35.31	-44.18	-44.17
5,20	-30.61	-39.57	-46.05	-42.89
10,20	-24.77	-43.74	-48.5	-42.25

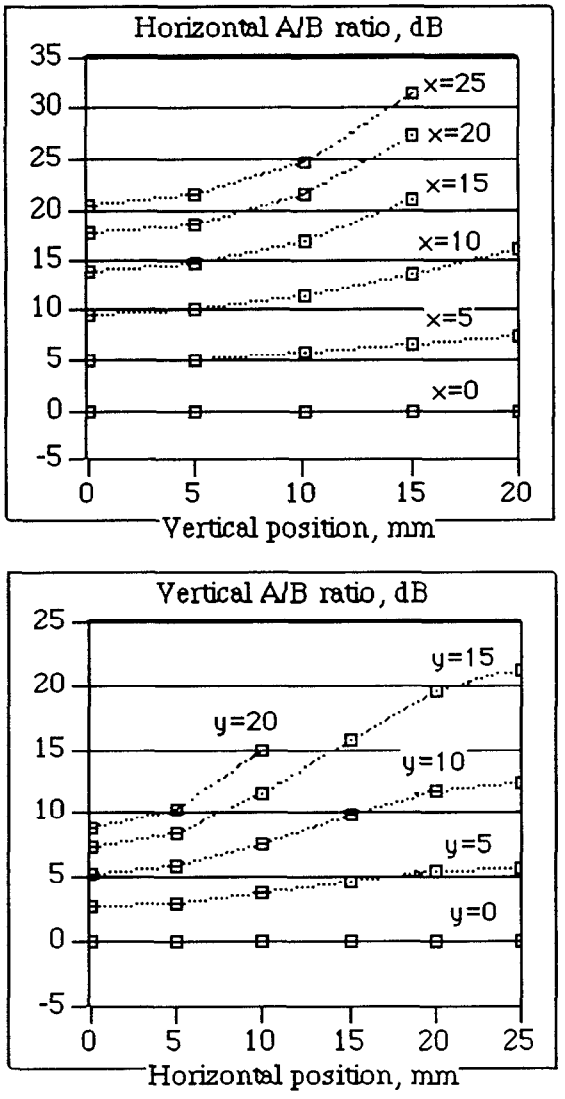

Figure 3. Simulated strip power outputs and ratios of combined powers for various beam positions. Strips #1,2,3,4 = top right, top left, bottom left, and bottom right. Table of output powers in dBm for beam at (x,y). Horizontal ratio = (1+4)/(2+3) dB, vertical ratio = (1+2)/(3+4) dB. Graphs show orthogonal and measured plane dependence.

The results from Figure 3 indicate beam position in the orthogonal plane has an appreciable effect. The existing Main Ring electronics will be reused in the FMI. Currently it is planned to instrument only one plane at each detector by measuring the ratio of combined pairs of plate outputs. If necessary, the measurement could be corrected with a two dimensional lookup table by deriving the orthogonal position from neighboring detectors. A study was performed to determine if this effect would be reduced by using a skew coordinate system[6].

The effect of beam size can be estimated by convolving the transverse beam distribution with the measured transfer function of detector and the response of the

electronics. For a gaussian shaped beam with emittance of 20π mm-mrad at 8 GeV, (σ_X = 3 mm), the error will be 0.75 mm when the beam is 20mm from center.

Wire measurements to verify the calculated response were performed. An HP8753B network analyzer was used to drive an open-ended 1/16 inch diameter wire placed inside the detector. The ratio of appropriately combined pairs of plates was measured as the wire was moved in 5 mm steps along the horizontal and vertical axis, (see Figure 4). The detector sensitivities are 1.1 dB/mm in the horizontal plane and 0.5 db/mm in the vertical. Measurements with wire positions off axis, not shown here, were in good agreement with Figure 3.

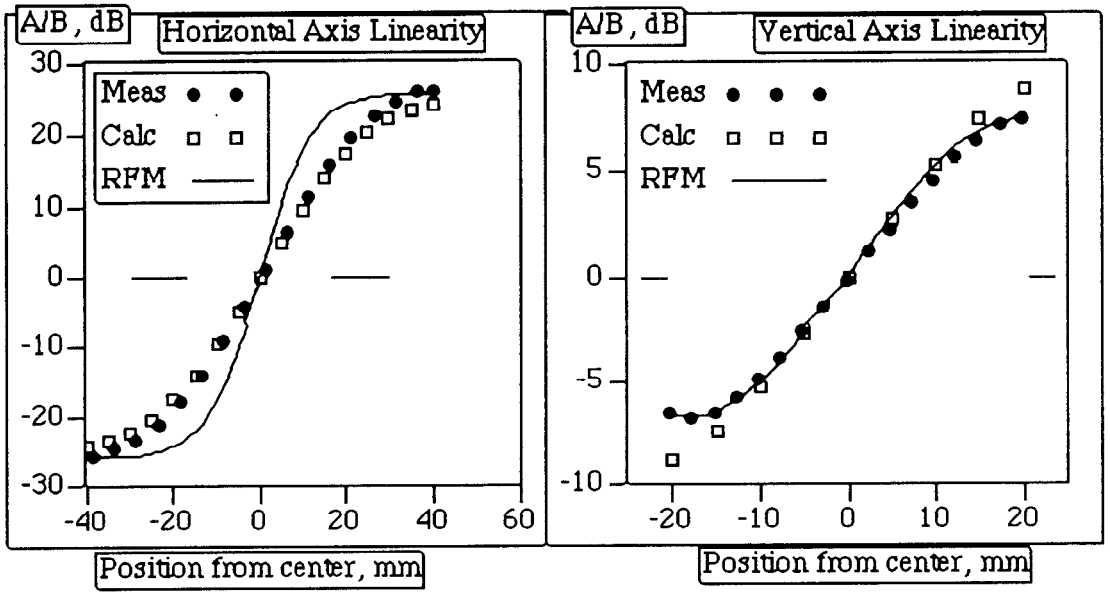

Figure 4. Prototype detector response along the axes, simulation and measurement. Strip projections onto the axes are shown for reference. Measured RF Module response (RFM) shown unscaled for comparison.

The FMI will reuse the existing Main Ring BPM system electronics. The RF Modules[7] isolate the 53 MHz component of the signal and apply the AM to PM conversion technique to extract the position. The output voltage from the A and B inputs can be estimated from the equation below.

$$V = \tan^{-1}\left\{\frac{A}{B}\right\} - \frac{\pi}{4}, \quad or \quad V = \tan^{-1}\left\{10^{\frac{(\%_B)_{dB}}{20}}\right\} - \frac{\pi}{4} \qquad (2)$$

The non-linearity of the arc tangent function can be seen in the RFM curve of Figure 4. In the existing Main Ring system, the linearity is corrected with a lookup table. The 8 bit conversion of the RF Module output results in decreased resolution as the beam moves off center. The resolution expected from the FMI detector is shown in Figure 5.

The characteristic impedance of the striplines was predicted with the simulation code by taking the cross section of the detector. The capacitance and inductance matrices of the four strips determine the impedances between the strips and ground. Measurement of the second prototype indicates a range of 45-53Ω among the four strips with as much as 3Ω variation along each strip. A gap variation

as small as ±5 mils can cause these differences. These combine with other mismatches and alignment errors to give an electrical offset to the detector. This is correctable in the processing, but variations along each strip and the mismatch to the output cables may affect beam impedance.

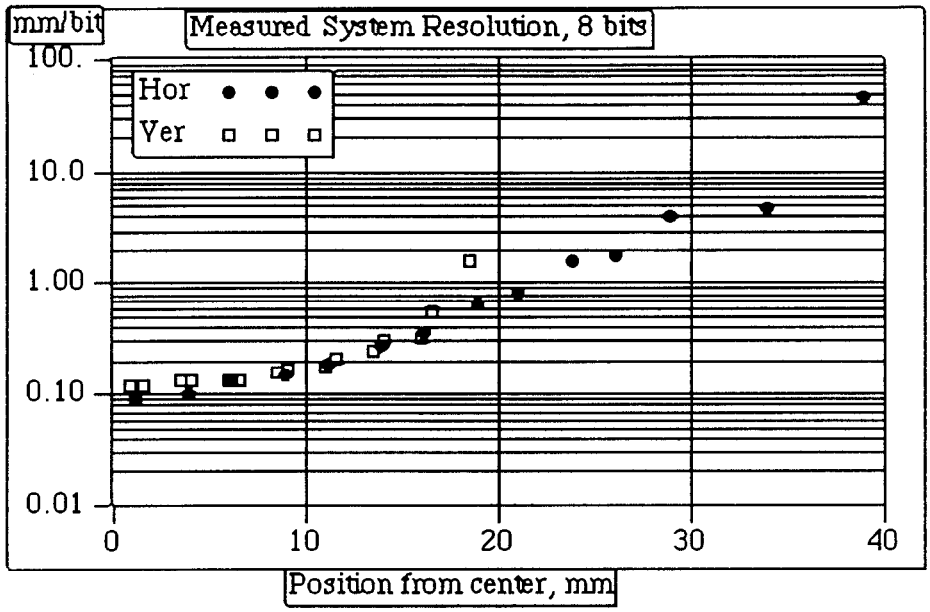

Figure 5. Measured system resolution of the FMI BPM system, including the prototype detector and the processing electronics (RF Module) for an 8 bit ADC. Measurements are taken along both axes. Multibunch beam is assumed.

The dynamic range of the electronics must accommodate ranges in beam current, position, and cable attenuation. Table 1 details the system power budget. The smallest input signal corresponds to the lowest amount of centered beam and the longest cable run. The normalized case corresponds to the second prototype detector and the beam conditions used in Figure 3. From the results, the 20 cm length of the second prototype has been determined to be electrically satisfactory. No additional amplification, attenuation, or switching circuitry is necessary.

Only a small portion of the detector signal spectrum is used for processing. The remaining spectral content presents two main concerns. First, beam impedance could be significantly increased by the 204 BPM systems. The RF Module provides a good cable termination for the harmonics of 53 MHz, which are present for continuous beam bunched at that frequency. However, parts of the transient beam spectrum could reflect back to the shorted detectors with a return loss as low as 5 dB. Calculations of beam impedance have commonly assumed matched terminations, but, in reality, large impedances could exist.

Second, beam at higher energies result in longitudinally shorter bunches. This results in higher detector output power, mainly at higher frequencies. Bunch length sigmas of 1.0 and 0.5 nsec add approximately +10 and +16 dB, respectively, to the 2 nsec case. This additional power can damage the RF Module's front end and limit the choices for the strip combiners. One possibility to be considered is a diplexer filter. The processed frequency is transmitted to the electronics while the remaining spectral content is terminated in a 50Ω load. By doing this, the beam impedance problem is also resolved. This circuit can be implemented easily with two inductors and two capacitors.

Table I Power budget for the FMI BPM system

Normalized 53 MHz power @ detector (1E9 ppb full ring, 2 nsec sigma bunch length, centered beam, strip width=0.5", d=0.919", length=20 cm, no cable loss)		-24.2 dBm
Beam Current range, ppb (continuous)	1E9-8E10	0-38.1 dB
Cable length, feet, RG8 cable (50 MHz)	150'-1150'	2-14 dB
Position differences, mm	(25,15)-(0,0)	0-10.7 dB
Minimum power @ RF Module, 53 MHz		-38.2 dBm
Maximum power @ RF Module, 53 MHz		+22.6 dBm
RF Module input power range		-35 to +27 dBm

CONCLUSION

Space restrictions in the Fermilab Main Injector has motivated the development of a detector which fits into the quadrupole magnets. Simulation code has proven useful in realizing desired specifications in a time efficient manner. A prototype detector that satisfies the requirements has been constructed and measured. Refinement of the design considering cost and reproducibility is in progress.

ACKNOWLEDGEMENTS

The authors would like to thank R. Meadowcroft and J. Arthur for their work on the detector prototypes, including assembly and measurements.

REFERENCES

1. Fermilab Main Injector Title 1 Design Report (1992), pp. 8-10.
2. D. E. Johnson, Proc. 4th Annual Workshop on Accel. Instrum., AIP 281, 291 (1992).
3. L. Sauer, Part. Acc. Conf. (1993), proceedings to be published.
4. A. Djordevic et al., Matrix Parameters for Multiconductor Transmission Lines (Artech House, Norwood, MS, 1989).
5. R. E. Shafer, Workshop on Accel. Instrum., AIP 212, 26 (1989).
6. P. J. Chou, Fermilab, unpublished.
7. S. P. Jachim, R. C. Webber, R. E. Shafer, IEEE Nucl. Sci. 28, 2323 (1981).